THE JOURNAL OF BONE & JOINT SURGERY

JB&JS

This is an enhanced PDF from The Journal of Bone and Joint Surgery

The PDF of the article you requested follows this cover page.

Spinal Hemiepiphysiodesis Decreases the Size of Vertebral Growth Plate Hypertrophic Zone and Cells

Donita I. Bylski-Austrow, Eric J. Wall, David L. Glos, Edgar T. Ballard, Andrea Montgomery and Alvin H. Crawford

J Bone Joint Surg Am. 2009;91:584-593. doi:10.2106/JBJS.G.01256

This information is current as of May 19, 2009

Supplementary material Commentary and Perspective, data tables, additional images, video clips and/or translated abstracts are available for this article. This information can be accessed at **http://www.ejbjs.org/cgi/content/full/91/3/584/DC1**

Reprints and Permissions Click here to **order reprints or request permission** to use material from this article, or locate the article citation on jbjs.org and click on the [Reprints and Permissions] link.

Publisher Information The Journal of Bone and Joint Surgery
20 Pickering Street, Needham, MA 02492-3157
www.jbjs.org

Copyright © 2009 by The Journal of Bone and Joint Surgery, Incorporated

Spinal Hemiepiphysiodesis Decreases the Size of Vertebral Growth Plate Hypertrophic Zone and Cells

By Donita I. Bylski-Austrow, PhD, Eric J. Wall, MD, David L. Glos, BSE, Edgar T. Ballard, MD, Andrea Montgomery, BS, and Alvin H. Crawford, MD

Investigation performed at the Division of Pediatric Orthopaedic Surgery, Cincinnati Children's Hospital Medical Center, Cincinnati, Ohio

Background: Hemiepiphysiodesis is a potential method to treat idiopathic juvenile scoliosis early. The purpose of the present study was to investigate a mechanism of curve creation in the pig thoracic model of spinal hemiepiphysiodesis by determining whether the structure of the vertebral growth plate varied with distance from the stapled, concave side of the spine. The hypotheses were that the heights of the hypertrophic zone, hypertrophic cells, and disc would be decreased on the treated side of the treated level as compared with both an unstapled control level and the side opposite the staple.

Methods: Custom spine staples were implanted into six midthoracic vertebrae in each of five skeletally immature pigs. After eight weeks, the spines were harvested and histological sections were prepared. Hypertrophic zone height, hypertrophic cell height and width, and disc height were measured at discrete coronal plane locations at stapled and unstapled thoracic levels. Differences between stapled and unstapled levels and locations were compared with use of mixed linear modeling for repeated measures, followed by regression models to determine growth plate intercept and slope across the plane by thoracic level.

Results: Zone height, cell height, and cell width were lowest on the stapled side of the stapled level, with significant differences in the overall statistical model ($p < 0.02$). Disc heights were significantly reduced ($p < 0.0001$) at the stapled levels across the coronal plane.

Conclusions: Unilateral control of intervertebral joint motion decreased growth plate height, cell size, and disc height.

Clinical Relevance: A method of spinal hemiepiphysiodesis with use of a clinically relevant procedure has been shown to create a gradient in growth plate structure. If a similar gradient can be produced in humans, mechanical growth modulation may prove capable of slowing or stopping the progression of early-stage spinal deformity.

Current surgical correction, instrumentation, and fusion techniques for spinal deformity in children and adolescents are invasive and may lead to adjacent-segment degeneration. Hemiepiphysiodesis has altered spine alignment in preclinical models[1-5] and therefore remains intriguing as a potential method of treating juvenile idiopathic scoliosis. Potential new treatments based on asymmetric inhibition of vertebral growth include the use of mechanical devices such as different types of staples[1-4,6,7], tethers[3-5,8], and screws[9]. The main mechanism of action is widely assumed to be slowed growth due to increased compression of the growth plate near the device, combined with continued growth of vertebrae on the contralateral side. However, an apparent spinal curvature may be caused by asymmetric compression of the disc rather than by altered vertebral growth.

Changes in mechanical loads alter growth plate structure and function. Experimental studies have shown clear histological and other biological changes in the physis due to stapling of the growth plates of long bones[10-18]. Spine growth alterations have been quantified after controlling displacement and loads

Disclosure: In support of their research for or preparation of this work, one or more of the authors received, in any one year, outside funding or grants in excess of $10,000 from Ethicon Endo-Surgery and DePuy AcroMed (now DePuy Spine) and less than $10,000 from the University of Cincinnati Women in Science and Engineering Fellowship. Neither they nor a member of their immediate families received payments or other benefits or a commitment or agreement to provide such benefits from a commercial entity. Commercial entities (DePuy Spine, Ethicon Endo-Surgery, and SpineForm) paid or directed in any one year, or agreed to pay or direct, benefits in excess of $10,000 to a research fund, foundation, division, center, clinical practice, or other charitable or nonprofit organization with which one or more of the authors, or a member of his or her immediate family, is affiliated or associated.

on rat tails[19,20]. Similar growth plate changes due to mechanical modifications have been reported in various species and anatomical locations[21,22]. The biomechanical environment of a growth plate especially affects the final volume and shape achieved by hypertrophic chondrocytes[12,17,23]. Cell volume and shape during hypertrophy substantially correlate with differences in growth rates[24,25]. Cell volume and shape are correlated with many biological factors, from structural protein production to genetic expression[12,15,23-29]. Clinically, the converse is widely known: the strength of the growth plate is sufficient to move and deform implanted devices[30]. For example, mechanical stresses generated by growth in the knees of adolescents have long been observed to bend staple blades[31-33].

In a previous report, spinal hemiepiphysiodesis with use of a staple-like implant was shown to induce asymmetric growth without fusion in skeletally immature, preadolescent porcine spines[1]. In that study, an anterior endoscopic approach was used without rib resection to produce a mean coronal plane spine curvature of 22° within eight weeks. In a pilot histological study that involved the use of an early implant design, chondrocyte hypertrophy appeared to be suppressed under the staple in comparison with the contralateral side. This finding suggested that increases in spinal curvature were likely attributable at least in part to structural changes to the growth plate.

The purpose of the present study was to investigate a mechanism of curve creation in the pig thoracic model of spinal hemiepiphysiodesis by determining whether the structure of the vertebral growth plate varied with distance from the stapled, concave side of the spine in the animals in the previous report[1]. The hypotheses were that the heights of the hypertrophic zone, hypertrophic cells, and disc would be decreased on the stapled side of the stapled level as compared with both an unstapled control level and the contralateral side.

Materials and Methods

Custom spine staples were implanted into the midthoracic region of the spine (Fig. 1) in seven live, skeletally immature female domestic pigs weighing 240 to 334 N (24 to 34 kg) with an age of three to four months. In the female pig, puberty occurs at five to six months and adolescence is considered to be between five and eighteen months. The procedures were approved by an Institutional Animal Care and Use Committee and complied fully with the Animal Welfare Act. The animals were maintained in adjacent, individual cages for the eight-week postoperative period, and they were confined except during cage cleaning. Six staples per pig were implanted into the left side of adjacent vertebrae from T6-T7 to T11-T12 with use of thoracoscopic procedures. After the animals were killed, the thoracic spines were harvested, the screws and staples were carefully removed, and the spines were stored frozen. Radiographic results have been previously described[1].

The purpose of the staples was to control displacement on one side of the intervertebral joint and thereby induce a compressive stress gradient across the joint. The staples were designed by two of the investigators (E.J.W. and D.I.B.-A.) and

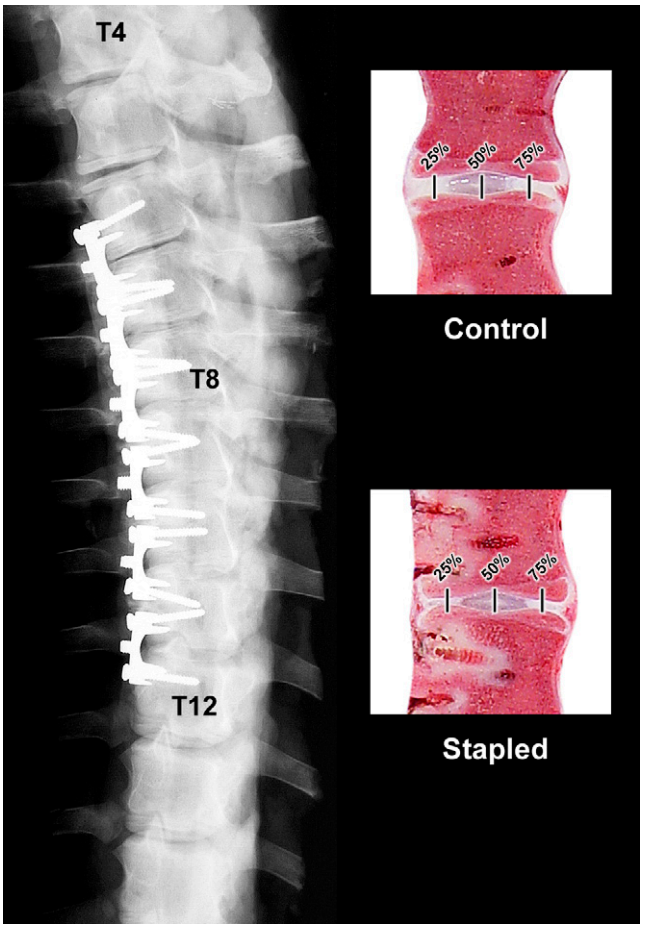

Fig. 1
Oblique radiograph (left) of a harvested porcine spine (Specimen 5), made eight weeks postoperatively, showing a true lateral view of the staples and the plane of maximum curvature. The insets on the right side of the image illustrate how disc heights were measured for all levels from T4 to T13 at 25%, 50%, and 75% of the distance from the staple to the contralateral cortex, as indicated by the lines on one control level (top) and one stapled level (bottom) from another animal (Specimen 3).

were fabricated of stainless steel (Techform Advanced Casting Technology, Portland, Oregon). A guidewire (a Kirschner wire with a 1.1-mm diameter) (MicroAire, Charlottesville, Virginia) was used to center the cannulated staples over the disc. Self-tapping stainless steel bone screws with a diameter of 2.7 mm and a length of 22 mm (Synthes, Monument, Colorado) were used to prevent the staples from backing out; two screws were used per staple.

The spines were thawed and were cut along the mid-coronal plane with a band saw. Digital photographic images of the entire thoracic cross-section were acquired from a distance of 0.9 m. The spines were then fixed in 10% neutral buffered formalin (Richard-Allan Scientific, Kalamazoo, Michigan). After complete fixation, the spines were decalcified (Decalcifier II; Surgipath Medical, Richmond, Illinois) in more than twenty

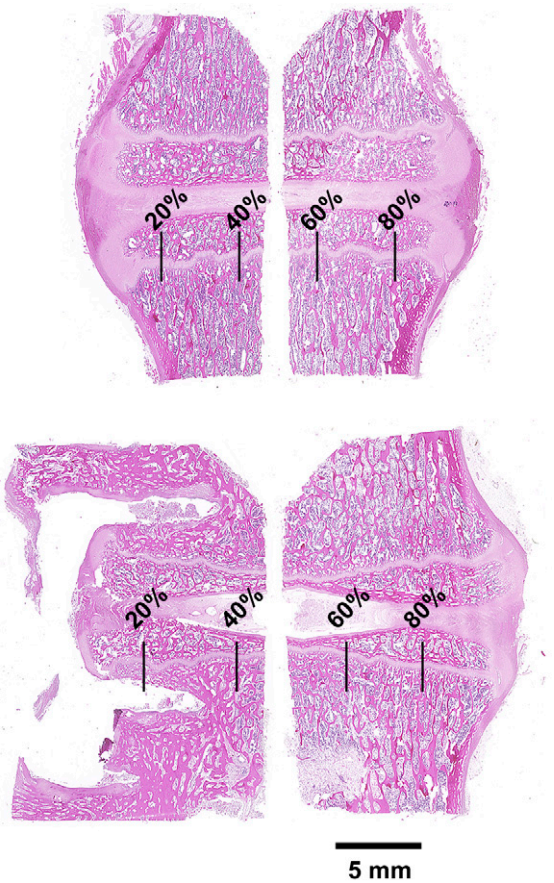

Fig. 2-A

Photomicrographs of coronal sections of two bisected vertebral motion segments from one animal (Specimen 5). The top section is from a control level (T4-T5), and the bottom section is from a stapled level (T8-T9); the staple has been removed from the left side at the stapled level. Lines overlying the end plates indicate the centers of the four sampling locations at 20%, 40%, 60%, and 80% of the distance from the staple to the contralateral cortex. The 20% location was directly between the staple blades (hematoxylin and eosin, ×100).

times the volume of the specimen. Two motion segments were resected and were split at the midsagittal plane. T4-T5 was chosen nominally as the unstapled control level, and T8-T9 was chosen as the treated level. Halved motion segments were embedded in paraffin and were sectioned parallel to the longitudinal axis of the spine at a thickness of 4 μm. Mounted sections were stained with hematoxylin and eosin (Fig. 2-A). Growth plate variables were measured at one physis per level. The cephalad or the caudad growth plate was chosen on the basis of which one exhibited better overall section quality. Digital images of the growth plates and a calibration scale were acquired with use of light transmission microscopy (nominal, ×100) and a digital camera. The sections were assembled into a composite microscopic image of each growth plate across the entire coronal plane. Growth plate variables were measured within four sampling locations located at 20%, 40%, 60%, and 80% of the distance from the staple to the contralateral cortex. At each of the four locations, variables were measured along a 1.5-mm linear distance, which defined the controlled sample space. The total vertebral width at the growth plate was approximately 26 mm, so that about one-quarter of the growth plate was sampled per level.

Qualitatively, differences between sampling locations were apparent, particularly between unstapled and stapled levels on the stapled side (Fig. 2-B). To quantify the differences, the height of the hypertrophic zone of the growth plate and the height and width of the cells within the zone were measured (Photoshop 7.0; Adobe Systems, San Jose, CA) (Fig. 3). The main variables of interest were the relative differences from side to side and from level to level within each spine. The hypertrophic zone was defined as the area in which chondrocytes were larger and lighter in comparison with those of the proliferative zone. Zone heights were measured along the longitudinal axis of the local growth plate boundaries in the direction of the cell columns. Only cells with clear boundaries were measured. The height of the hypertrophic zone was defined as the distance from the top edge of the most cranial cell to the bottom edge of the most cephalad cell. About fifty zone heights were measured for each sampling location, or 200 per level, at approximately equally spaced intervals.

Cell heights were aligned with the local zone height direction (Fig. 3). The width of each cell was defined as the largest left-to-right distance orthogonal to cell height. Only cells within the hypertrophic zone and with distinct boundaries were mea-

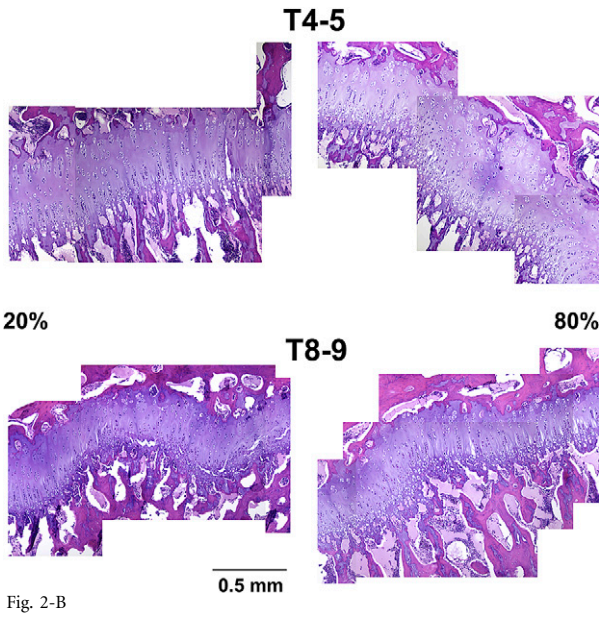

Fig. 2-B

Photomicrographs of growth plate sample sections from the control level T4-T5 (top) and the stapled level T8-T9 (bottom) from the stapled side (20%) and the unstapled side (80%) from one animal (Specimen 5). The vertebral body is toward the bottom of each section (hematoxylin and eosin, ×100).

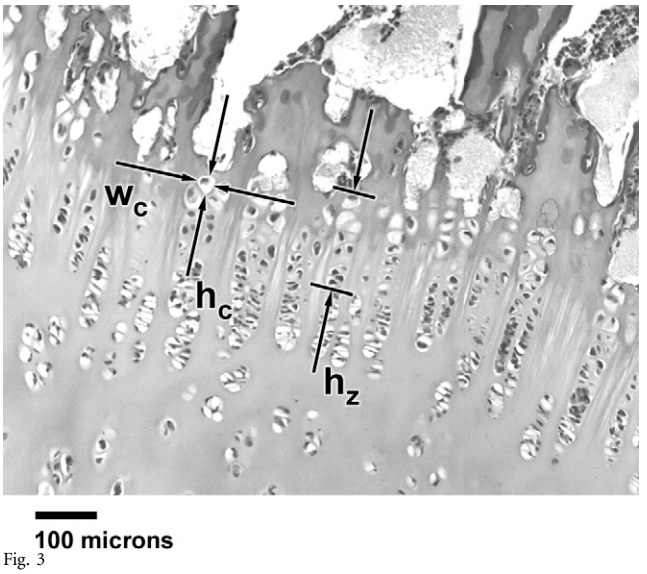

Fig. 3

Within each sampling location, three growth plate variables were measured: the height of the hypertrophic zone (h_z) and the height (h_c) and width (w_c) of the cells within the hypertrophic zone. The height of the hypertrophic zone was defined as the distance from the top edge of the most cephalad qualifying cell to the bottom edge of the most caudad one. The directions and magnitudes of each dimension are shown by the arrows.

sured. Every eligible cell was included, regardless of size, with no attempt to discern bisected cells, for a total of approximately 200 cells per location, or 800 per vertebra.

Disc heights were measured from the digital images of the gross cross sections with use of commercial software (Photoshop 7.0). Every disc was measured at nine levels, from T4-T5 to T12-T13 inclusive, at three locations in the plane: 25%, 50%, and 75% of the distance from the staple to the contralateral cortex (Fig. 1, insets).

Statistical Methods

Mixed linear modeling for repeated measures[34,35] was performed with use of three factors: animal (Specimens 1 through 5), thoracic level (stapled or unstapled), and coronal plane location (20%, 40%, 60%, 80%). The null hypotheses were that the outcome variables were not different between the stapled and unstapled thoracic levels and across the coronal plane locations. Separate tests were conducted for the dependent variables of zone height, cell height, cell width, and disc height. When significant differences were found for the interaction ($p < 0.05$) in the overall model, the Bonferroni correction was used. For growth plate variables, the significance level to test for differences between locations was 0.0125 (0.05/4), because only the differences between stapled and unstapled levels at corresponding locations were of interest, e.g., the difference between the two 20% locations. When left-to-right-side differences in disc height were compared, the significance level was 0.025 (0.05/2).

Next, regression models were separately fitted, again with use of a mixed modeling process, to stapled and unstapled levels in order to test whether each slope was different from zero. The dependent variables were zone height, cell height, and cell width, and the independent variable was coronal plane

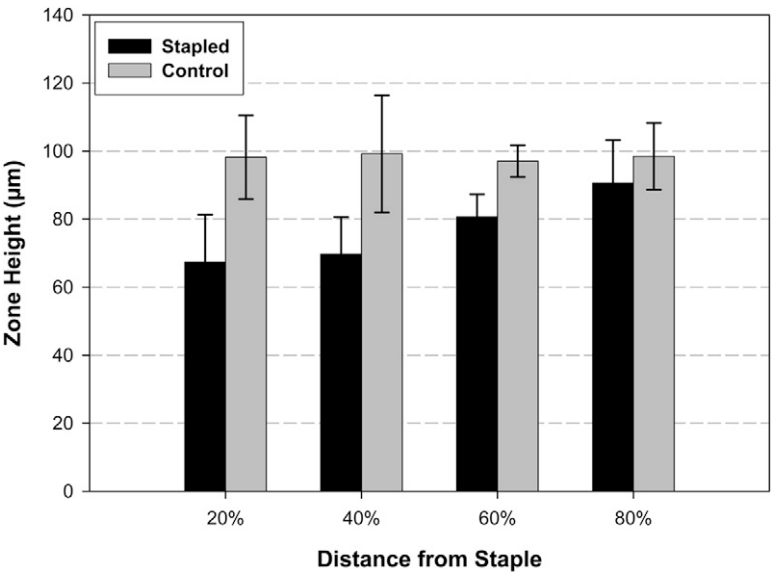

Fig. 4

Hypertrophic zone height (shown as the mean and the standard deviation based on five specimens) varied according to level (stapled as compared with unstapled control) and according to the normalized distance from the staple across the plane at the stapled level. A distance from the staple of 100% corresponds to the far right cortex, whereas a distance of 20% indicates the sampling location directly between the staple blades.

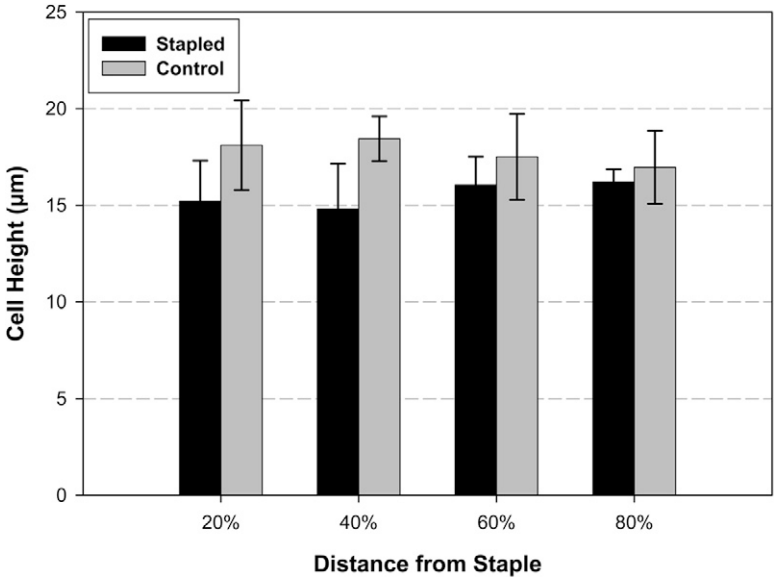

Fig. 5-A

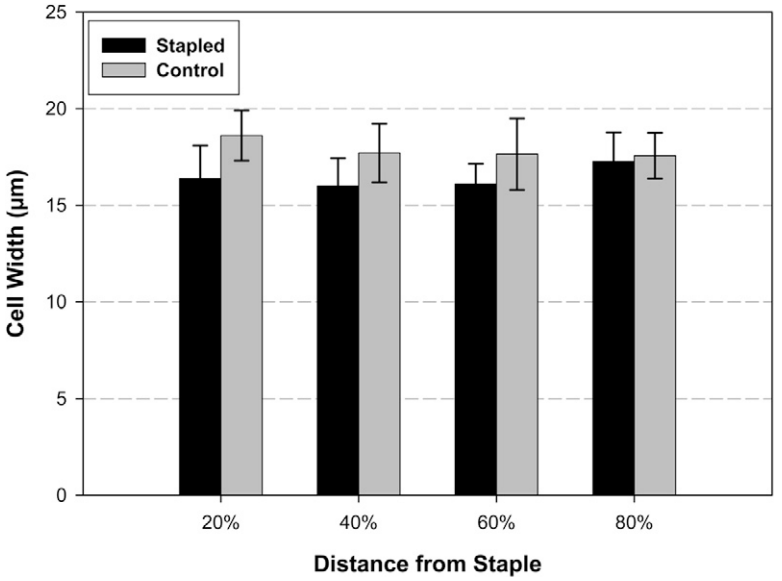

Fig. 5-B

Fig. 5-A Hypertrophic cell height (shown as the mean and the standard deviation based on five specimens) varied according to level (stapled as compared with unstapled control). **Fig. 5-B** Hypertrophic cell width (shown as the mean and the standard deviation based on five specimens) varied according to level (stapled as compared with unstapled control).

location. The intercept was the value of the dependent variable at the left edge of the vertebra, which would correspond to a coronal plane location of 0%. The slope was the rate of change of the dependent variable as a function of normalized distance from the left edge of the vertebra (coronal plane location, 0%) to the right edge (coronal plane location, 100%). The p values for slopes indicate the probability that the slope was equal to zero, i.e., the probability that the dependent variable was constant across the coronal plane. The significance level to test if slopes at the stapled and unstapled levels were different from zero was 0.025 (0.05/2).

Source of Funding

Funds from DePuy AcroMed (now DePuy Spine) were provided to conduct the surgical portion of the study at Ethicon Endo-Surgery, Inc., and were used for animal purchase and per diems, surgical supplies, and veterinary technical support. No funds were transferred to any author or to the authors' institution. Funds for student salary for one author (A.M.) were provided by the Women in Science and Engineering Program of the University of Cincinnati.

Results

Five animals completed the eight-week protocol and were included in the analysis. Of the other two animals, one died two days postoperatively with hemorrhage of the costal vasculature and the other exhibited asymmetric movement of the hind limbs after surgery and failed to gain weight for six weeks. Gastric ulcers were found at the time of the autopsy. These two animals were eliminated from further analysis. The remaining

TABLE I Differences Between Corresponding Coronal Plane Locations at Unstapled and Stapled Thoracic Levels for the Three Dependent Growth Plate Structural Variables

	Zone Height		Cell Height		Cell Width	
Coronal Location	Difference (*μm*)	P Value	Difference (*μm*)	P Value	Difference (*μm*)	P Value
20%	31.2	0.0001*	2.66	0.0001*	2.32	0.0001*
40%	29.6	0.0001*	2.94	0.0001*	0.90	0.0001*
60%	15.7	0.0001*	1.14	0.0001*	1.29	0.0001*
80%	10.7	0.0001*	0.82	0.0001*	0.41	0.0291

*Significant ($p < 0.0125$).

animals gained an average of 142% of their weight as measured at the time of surgery. The thoracic levels used for growth plate measurements (see Appendix) varied from the protocol by as many as two levels in two animals because of variations in staple placement and the number of thoracic levels removed at the time of harvest. Hypertrophic zone height (Fig. 4), cell height (Fig. 5-A), and cell width (Fig. 5-B) were all lowest on the stapled side of the stapled level. All three growth plate variables showed significant differences in the overall model ($p < 0.02$). The disc heights (Fig. 6) of stapled vertebrae were significantly less than those at unstapled levels ($p < 0.0001$) across the entire coronal plane.

The mean zone height, across the four coronal plane locations, of the unstapled control level was 98.2 μm, whereas that of the stapled level was 77.1 μm. The mean zone height under the staple was 69% of the control zone height and 74% of the zone height on the contralateral side. At the stapled level, the zone height on the side contralateral to the staple was 92% of the mean control zone height (Fig. 4). Zone heights at corresponding coronal plane locations were significantly different from each other (Table I). Zone height was directly related to distance from the staple at the treated level (Table II), whereas zone height at the control level did not vary across the plane.

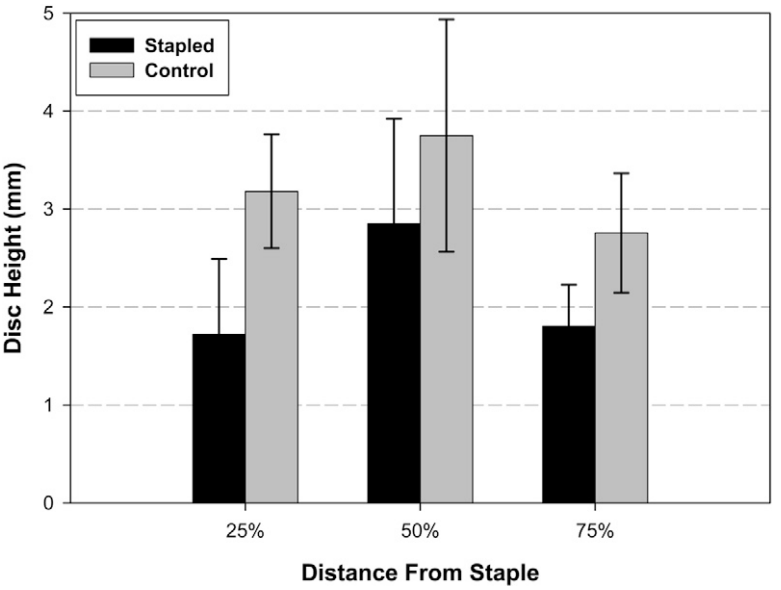

Fig. 6

Intervertebral disc height (shown as the mean and the standard deviation based on five specimens) varied according to level (stapled as compared with unstapled control). However, differences according to the distance from the staple were due to the greater height of the disc nucleus at the central sampling location (50%) as compared with the heights at both the stapled, left side (25%) and the unstapled, right side (75%) rather than to the differences between the two anular heights.

TABLE II Intercept and Slope for Each Growth Plate Variable as a Function of the Normalized Coronal Plane Location by Thoracic Level

	Stapled Thoracic Level			Unstapled Thoracic Level		
	Intercept (μm)	Slope (μm/%)	P Value†	Intercept (μm)	Slope (μm/%)	P Value†
Zone height	58.5	0.36	0.0021*	98.6	−0.0069	0.95
Cell height	14.4	0.023	0.154	18.8	−0.022	0.26
Cell width	15.8	0.014	0.32	18.7	−0.016	0.28

*Significant ($p < 0.025$). †P values indicate the probability that the slope is different than zero.

The average number of cells measured per animal was 1558 ± 201, with no significant difference between stapled and unstapled levels ($p > 0.1$). The mean cell heights of the control and stapled levels were 17.8 and 15.5 μm, respectively. The mean cell height, across the four coronal plane locations, under the staple was 85% of the control value and 93% of the value on the contralateral side, whereas the value on the contralateral side of the stapled level was 91% of the control value (Fig. 5-A). Cell height varied between stapled and control levels. Cell heights at corresponding coronal plane locations were significantly different from each other (Table I). The slopes at unstapled and stapled levels were not significantly different from zero (Table II).

The mean cell width, across the four coronal plane locations, was 17.9 μm at the control level and 16.4 at the stapled level. The mean cell width under the staple was 91% of the control value and 94% of the value on the contralateral side. The value on the contralateral side of the stapled level was 97% of the control value (Fig. 5-B). Cell widths at corresponding coronal plane locations were significantly different from each other, with the exception of the right side (80%) locations (Table I). The slopes at unstapled and stapled levels were not significantly different from zero (Table II).

Mean disc heights, across the four coronal plane locations, were lower at the stapled levels (2.1 mm) than at the control levels (3.2 mm) ($p < 0.0001$). The disc height under the staple was 58% of the control value, whereas the height on the contralateral side was 61% of the control value (Fig. 6). At unstapled levels, the side-to-side difference in the height of the disc anulus (0.42 mm) was significant ($p = 0.008$), with the height of the anulus on the contralateral, unstapled side being smaller than that on the ipsilateral side.

Discussion

Spinal hemiepiphysiodesis with use of a staple-like implant induced structural changes in the hypertrophic zone of the growth plate and in the intervertebral disc. Growth plate hypertrophic zone height was related to the presence of the staple and the distance from the staple. On the stapled, concave side of the thoracic spine, hypertrophic zone height and cell height and width were significantly smaller[36]. Structural changes were consistent with increased compression of both the disc and the growth plates. These results support the concept of a compression gradient being at least a part of the mechanism of graduated growth inhibition, as is widely presumed to be the case for epiphyseal staples in the treatment of lower limb deformities. Growth plate structural changes were greatest under the staple and diminished across the coronal plane to nearly control levels. Cell width was decreased in addition to cell height, so chondrocytes did not expand laterally to maintain a constant volume or to grow perpendicular to the applied stress direction.

Limitations in the experimental design included a relatively small sample size, one evaluation time, grouped means at each of four sampling locations, a quadruped model, and the use of unstapled levels in treated animals as controls. Control physis measures may vary by level so that differences between the control level and the more caudad treated level may be due, in part, to a gradient by thoracic level. It is not known how much T4-T5 normally differs from T8-T9. The possibility of compensatory curves at the unstapled levels was a limitation of using unstapled levels as controls. Associated changes in vascular and other structures were not differentiated in the present study, and pressure effects have been hypothesized to act through changes to the blood supply, with similar histological effects[37].

The effects of piercing the disc with a guidewire during the surgical procedures and the effects of vascular or other biological changes[38,39] may not be isolated from the effects of compression in the present study, and no surgical sham was performed. Disc puncture in isolation has been used as a model of mild disc degeneration[40]. Biological and biomechanical effects due to disc compression[41-54] and due to puncture of the anulus[40,55,56] have been reported. In the current study, a guidewire was convenient but was not required, and one was not used in subsequent experiments. The controlled mechanical variable, intervertebral joint displacement on the stapled side, was not measured. Joint motion was assumed to be zero at the staple base given that the base was essentially infinitely stiff compared with the disc. Displacements of the intervertebral joint would be expected to be small within the blades and to increase with distance from the staple.

Technical limitations included relatively simple tissue processing and structural measurements. Variations in the number of ribs, the location of the staples, and section quality resulted in some differences in terms of which levels were used for growth plate measurements. The instrumentation was relatively easy to remove, and gross tissue sections did not contain

evidence that the removal of staples and screws affected the morphology near any sampling location. The histomorphometry methods did not yield absolute zone and cell sizes. The process of fixing and decalcifying paraffin-embedded bone samples is well known to cause tissue shrinkage and morphologic changes[28,57], and no attempt was made to measure only cells cut at midplane. The location of the sectioning plane relative to the midline of the staple varied both between spines and between levels. The sections cut closest to the midline of the staple exhibited the greatest differences in growth plate variables compared with controls. All sections were used in the analysis, not only those that were cut most closely to the staple midline. More consistent section plane locations may have yielded more significant differences across the coronal plane. Sectioning artifacts included fissures in the growth plate. Artifacts were judged to be relatively mild and were managed with the use of redundant slides and the ability to choose either the cephalad or caudad growth plate. Because the zone heights on the stapled side and level were smaller, the total area and volume of the stapled locations were decreased. Therefore, the length of each location was chosen as the controlled space to provide a spatial reference basis for sampling that was independent of treatment and location. Growth plate height measurements were performed twice, with the second study reproducing the patterns of the first with smaller variances.

Disc heights were measured unloaded and after cutting and so were not necessarily comparable with uncut or in vivo heights. Again, paired differences between level and side were the goal. A calibration photograph showed no measurable change in calibration factor along the spine section. Disc heights were measured twice by different observers, with no changes in any statistical conclusion.

The results of the present study may be compared with those of studies of tissues routinely processed after autopsy in humans[58]. Corresponding measurements from patients with scoliosis may help to quantify the potential for growth inhibition in humans. A preliminary report of hypertrophic zone and cell heights in humans[58] indicated that they may be smaller than those of animal models. Other limitations in the ability to translate the results to possible human use include both global and local anatomical and biomechanical differences between species. However, comparisons between the biomechanical properties[59] of quadruped and biped spines, and similarities across species in the dose-response curve of the growth plate to compression[22], support at least in part the relevance of the study to human vertebrae. Normal physiological compressive stresses in the porcine spine are likely approximately half of those in the human spine[60].

While tissue processing, definitions of variables and controls, and other experimental differences will affect quantitative results, zone and cell height reductions due to treatment may be compared with relative values from studies on other animal models[17-20,22]. In one study, staples were placed across the proximal tibial growth plate of four-week-old rats for fourteen days[18]. Under the staple, growth decreased to 33% of the control value, whereas on the side furthest from the staple, growth was 85% of the control value. In another study, growth rate differences in the spine that were produced by sustained mechanical loading of rat tail vertebrae were associated with reductions in the expected height increases of hypertrophic chondrocytes in the direction of growth[20]. After four weeks with an applied compressive load of 60% of body weight (1.2 N; nominal stress, 0.1 MPa), the average zone height and cell height in compressed tail vertebrae were 87% and 85%, respectively, of control values. With respect to disc height, another study of rat tails[44] demonstrated that after eight weeks with applied compressive loads of up to 100% of body weight, or approximately 0.15 MPa above physiological stress, disc heights were reduced by nearly 50%. In a preliminary report of in vivo compressive stresses in the porcine disc, the static mean stress was increased 0.1 to 0.2 MPa following staple implantation[61].

Results from a study of pigs would presumably be most directly applicable to humans if the growth rates were similar. However, human spinal growth rates are quite slow. A comparison of growth rates between the two species would be needed to interpret and translate the results. The increase in length of the thoracic spine (T2 to T12) in domestic pigs from the initial age to the final age in the present study was approximately 7 cm, which corresponds to an average growth rate of 50 μm per physis per day. The average remaining thoracic spine growth is approximately 7 cm in girls with a skeletal age of six years[62], and the average growth rate in children and adolescents is on the order of 1 μm per physis per day [22,63,64]. Therefore, while the growth rate of the pig is much faster than that of the human, the duration of growth is much shorter, so the total growth of the spine is similar. In clinical use, the assumption is that if treatment occurs sufficiently early and is in place long enough, the treatment effect is likely to be similar.

In conclusion, a method of spinal hemiepiphysiodesis that was previously reported to cause curvatures in an inverse analog treatment model altered vertebral growth plate structure in a porcine animal model consistent with transmission of compressive stress to the physes. The results of the present study support the concepts that scoliosis progression involves a compressive stress gradient and asymmetrically decreasing vertebral growth in a positive feedback control loop[65,66] and that an early developing scoliotic curve may be slowed by differential inhibition of the growth plate.

Appendix

eA A table showing section locations and growth plate variables for each specimen is available with the electronic versions of this article, on our web site at jbjs.org (go to the article citation and click on "Supplementary Material") and on our quarterly CD/DVD (call our subscription department, at 781-449-9780, to order the CD or DVD). ■

NOTE: Financial support was provided by DePuy AcroMed (now DePuy Spine), for the surgical portion of the study, and by the Cincinnati Children's Hospital Research Foundation. Laboratory support was provided by Ethicon Endo-Surgery, Inc.; special thanks to Ronald J. Kolata, DVM, and engineer Anthony Sexton. The design and fabrication of the collet-based endoscopic screwdriver is attributed to Arthur Case and Daniel Radigan (April 2001) of 7 Letters, Cincinnati, Ohio. Technical

assistance by David Sheyn, Jonathan Henkel, Alison Grimaldi, and Keith Stringer, MD, and statistical consultation by Judy Bean, PhD, are gratefully acknowledged.

Donita I. Bylski-Austrow, PhD
Eric J. Wall, MD
David L. Glos, BSE
Edgar T. Ballard, MD
Andrea Montgomery, BS
Alvin H. Crawford, MD
Cincinnati Children's Hospital Medical Center,
3333 Burnet Avenue,
Cincinnati,
OH 45229-3039.
E-mail address for D.I. Bylski-Austrow:
Donita.Bylski-Austrow@cchmc.org

References

1. Wall EJ, Bylski-Austrow DI, Kolata RJ, Crawford AH. Endoscopic mechanical spinal hemiepiphysiodesis modifies spine growth. Spine. 2005;30:1148-53.

2. Braun JT, Ogilvie JW, Akyuz E, Brodke DS, Bachus KN. Fusionless scoliosis correction using a shape memory alloy staple in the anterior thoracic spine of the immature goat. Spine. 2004;29:1980-9.

3. Braun JT, Akyuz E, Ogilvie JW, Bachus KN. The efficacy and integrity of shape memory alloy staples and bone anchors with ligament tethers in the fusionless treatment of experimental scoliosis. J Bone Joint Surg Am. 2005;87:2038-51.

4. Braun JT, Akyuz E, Udall H, Ogilvie JW, Brodke DS, Bachus KN. Three-dimensional analysis of 2 fusionless scoliosis treatments: a flexible ligament tether versus a rigid-shape memory alloy staple. Spine. 2006;31:262-8.

5. Newton PO, Fricka KB, Lee SS, Farnsworth CL, Cox TG, Mahar AT. Asymmetrical flexible tethering of spine growth in an immature bovine model. Spine. 2002;27:689-93.

6. Betz RR, Kim J, D'Andrea LP, Mulcahey MJ, Balsara RK, Clements DH. An innovative technique of vertebral body stapling for the treatment of patients with adolescent idiopathic scoliosis: a feasibility, safety, and utility study. Spine. 2003;28:S255-65.

7. Betz RR, D'Andrea LP, Mulcahey MJ, Chafetz RS. Vertebral body stapling procedure for the treatment of scoliosis in the growing child. Clin Orthop Relat Res. 2005;434:55-60.

8. Lowe TG, Wilson L, Chien JT, Line BG, Klopp L, Wheeler D, Molz F. A posterior tether for fusionless modulation of sagittal plane growth in a sheep model. Spine. 2005;30 (17 Suppl):S69-74.

9. Coillard C, Rhalmi S, Rivard CH. [Experimental scoliosis in the minipig: study of vertebral deformations]. Ann Chir. 1999;53:773-80. French.

10. Goff CW. Histologic arrangements from biopsies of epiphyseal plates of children before and after stapling. Correlated with roentgenographic studies. Am J Orthop. 1967;9:87-9.

11. Hall-Craggs EC, Lawrence CA. The effect of epiphysial stapling on growth in length of the rabbits tibia and femur. J Bone Joint Surg Br. 1969;51:359-65.

12. Ehrlich MG, Mankin HJ, Treadwell BV. Biochemical and physiological events during closure of the stapled distal femoral epiphyseal plate in rats. J Bone Joint Surg Am. 1972;54:309-22.

13. Christensen NO. Growth arrest by stapling. An experimental study of longitudinal bone growth and morphology of the growth region. Acta Orthop Scand Suppl. 1973:3-78.

14. Herwig J, Schmidt A, Matthiab HH, Kleeman H, Buddecke E. Biochemical events during stapling of the proximal tibial epiphyseal plate in pigs. Clin Orthop Relat Res. 1987;218:283-9.

15. Karbowski A, Camps L, Matthiass HH. Histopathological features of unilateral stapling in animal experiments. Arch Orthop Trauma Surg. 1989;108:353-8.

16. Farnum CE. Differential growth rates of long bones. In: Hall BK, editor. Bone. Volume 8: Mechanisms of bone development and growth. Boca Raton, FL: CRC Press; 1994. p 193-222.

17. Farnum CE, Wilsman NJ. Effects of distraction and compression on growth plate function. In: Buckwalter JA, Ehrlich MG, Sandell LJ, Trippel SB, editors. Skeletal growth and development: clinical issues and basic science advances. Rosemont, IL: American Academy of Orthopaedic Surgeons; 1998. p 517-32.

18. Farnum CE, Nixon A, Lee AO, Kwan DT, Belanger L, Wilsman NJ. Quantitative three-dimensional analysis of chondrocytic kinetic responses to short-term stapling of the rat proximal tibial growth plate. Cells Tissues Organs. 2000;167:247-58.

19. Mente PL, Aronsson DD, Stokes IA, Iatridis JC. Mechanical modulation of growth for the correction of vertebral wedge deformities. J Orthop Res. 1999;17:518-24.

20. Stokes IA, Mente PL, Iatridis JC, Farnum CE, Aronsson DD. Enlargement of growth plate chondrocytes modulated by sustained mechanical loading. J Bone Joint Surg Am. 2002;84:1842-8.

21. Ohashi N, Robling AG, Burr DB, Turner CH. The effects of dynamic axial loading on the rat growth plate. J Bone Miner Res. 2002;17:284-92.

22. Stokes IA, Aronsson DD, Dimock AN, Cortright V, Beck S. Endochondral growth in growth plates of three species at two anatomical locations modulated by mechanical compression and tension. J Orthop Res. 2006;24:1327-34.

23. Buckwalter JA, Mower D, Ungar R, Schaeffer J, Ginsberg B. Morphometric analysis of chondrocyte hypertrophy. J Bone Joint Surg Am. 1986;68:243-55.

24. Breur GJ, VanEnkevort BA, Farnum CE, Wilsman NJ. Linear relationship between the volume of hypertrophic chondrocytes and the rate of longitudinal bone growth in growth plates. J Orthop Res. 1991;9:348-59.

25. Wilsman NJ, Farnum CE, Leiferman EM, Fry M, Barreto C. Differential growth by growth plates as a function of multiple parameters of chondrocytic kinetics. J Orthop Res. 1996;14:927-36.

26. Buckwalter JA, Mower D, Schafer J, Ungar R, Ginsberg B, Moore K. Growth-plate-chondrocyte profiles and their orientation. J Bone Joint Surg Am. 1985; 67:942-55.

27. Klein-Nulend J, Veldhuijzen JP, Burger EH. Increased calcification of growth plate cartilage as a result of compressive force in vitro. Arthritis Rheum. 1986;29:1002-9.

28. Hunziker EB, Schenk RK. Physiological mechanisms adopted by chondrocytes in regulating longitudinal bone growth in rats. J Physiol. 1989;414:55-71.

29. Ehrlich MG, Armstrong AL. The role, characterization, and localization of physeal stromelysin. In: Buckwalter JA, Ehrlich MG, Sandell LJ, Trippel SB, editors. Skeletal growth and development. Rosemont, IL: American Academy of Orthopaedic Surgeons; 1998. p 241-52.

30. Safran MR, Eckardt JJ, Kabo JM, Oppenheim WL. Continued growth of the proximal part of the tibia after prosthetic reconstruction of the skeletally immature knee. Estimation of the minimum growth force in vivo in humans. J Bone Joint Surg Am. 1992;74:1172-9.

31. Blount WP, Zeier F. Control of bone length. J Am Med Assoc. 1952;148:451-7.

32. Bylski-Austrow DI, Wall EJ, Rupert MP, Roy DR, Crawford AH. Growth plate forces in the adolescent human knee: a radiographic and mechanical study of epiphyseal staples. J Pediatr Orthop. 2001;21:817-23.

33. Bylander B, Hansson LI, Selvik G. Pattern of growth retardation after Blount stapling: a roentgen stereophotogrammetric analysis. J Pediatr Orthop. 1983;3: 63-72.

34. Littell RC, Stroup WW, Wolfinger RD, Milliken GA. SAS system for mixed models. Cary, NC: SAS Institute; 1996.

35. Latour D, Littell R. Advanced general linear models with an emphasis on mixed models. Cary, NC: SAS Institute; 1996.

36. Bylski-Austrow DI, Wall EJ, Glos DL, Ballard ET, Stringer K, Crawford AH. Spinal hemiepiphysiodesis correlates with physeal histomorphometric gradients. In: Uyttendaele D, Dangerfield PH, editors. Research into spinal deformities 5. Amsterdam: IOS Press; 2006. p 261-6.

37. Trueta J, Amato VP. The vascular contribution to osteogenesis. III. Changes in the growth cartilage caused by experimentally induced ischaemia. J Bone Joint Surg Br. 1960;42:571-87.

38. Bibby SR, Fairbank JC, Urban MR, Urban JP. Cell viability in scoliotic discs in relation to disc deformity and nutrient levels. Spine. 2002;27:2220-8.

39. Bibby SR, Jones DA, Ripley RM, Urban JP. Metabolism of the intervertebral disc: effects of low levels of oxygen, glucose, and pH on rates of energy metabolism of bovine nucleus pulposus cells. Spine. 2005;30:487-96.

40. Masuda K, Aota Y, Muehleman C, Imai Y, Okuma M, Thonar EJ, Andersson GB, An HS. A novel rabbit model of mild, reproducible disc degeneration by an anulus needle puncture: correlation between the degree of disc injury and radiological and histological appearances of disc degeneration. Spine. 2005;30:5-14.

41. Lotz J, Colliou O, Chin J, Duncan NA, Liebenberg E. Compression-induced degeneration of the intervertebral disc: an in vivo mouse model and finite-element study. Spine. 1998;23:2493-506.

42. Lotz JC, Chin JR. Intervertebral disc cell death is dependent on the magnitude and duration of spinal loading. Spine. 2000;25:1477-83.

43. Walsh AJ, Lotz JC. Biological response of the intervertebral disc to dynamic loading. J Biomech. 2004;37:329-37.

44. Iatridis JC, Mente PL, Stokes IA, Aronsson DD, Alini M. Compression-induced changes in intervertebral disc properties in a rat tail model. Spine. 1999;24: 996-1002.

45. Iatridis JC, MacLean JJ, Roughley PJ, Alini M. Effects of mechanical loading on intervertebral disc metabolism in vivo. J Bone Joint Surg Am. 2006;88 Suppl 2:41-6.

46. Ching CT, Chow DH, Yao FY, Holmes AD. The effect of cyclic compression on the mechanical properties of the inter-vertebral disc: an in vivo study in a rat tail model. Clin Biomech (Bristol, Avon). 2003;18:182-9.

47. Kroeber MW, Unglaub F, Wang H, Schmid C, Thomsen M, Nerlich A, Richter W. New in vivo animal model to create intervertebral disc degeneration and to investigate the effects of therapeutic strategies to stimulate disc regeneration. Spine. 2002;27:2684-90.

48. MacLean JJ, Lee CR, Grad S, Ito K, Alini M, Iatridis JC. Effects of immobilization and dynamic compression on intervertebral disc cell gene expression in vivo. Spine. 2003;28:973-81.

49. MacLean JJ, Lee CR, Alini M, Iatridis JC. Anabolic and catabolic mRNA levels of the intervertebral disc vary with the magnitude and frequency of in vivo dynamic compression. J Orthop Res. 2004;22:1193-200.

50. Kasra M, Goel V, Martin J, Wang ST, Choi W, Buckwalter J. Effect of dynamic hydrostatic pressure on rabbit intervertebral disc cells. J Orthop Res. 2003; 21:597-603.

51. Hutton WC, Toribatake Y, Elmer WA, Ganey TM, Tomita K, Whitesides TE. The effect of compressive force applied to the intervertebral disc in vivo. A study of proteoglycans and collagen. Spine. 1998;23:2524-37.

52. Hutton WC, Elmer WA, Boden SD, Hyon S, Toribatake Y, Tomita K, Hair GA. The effect of hydrostatic pressure on intervertebral disc metabolism. Spine. 1999; 24:1507-15.

53. Urban JP. The chondrocyte: a cell under pressure. Br J Rheumatol. 1994; 33:901-8.

54. Ohshima H, Urban JP, Bergel DH. Effect of static load on matrix synthesis rates in the intervertebral disc measured in vitro by a new perfusion technique. J Orthop Res. 1995;13:22-9.

55. Aota Y, Masuda K, Nguyen C, Andersson GB, Thonar E, An HS. Radiological and MRI analyses of a novel rabbit model: a mild, progressive disc degeneration. Trans Orthop Res Soc. 2002;27:118.

56. Singh K, Masuda K, An HS. Animal models for human disc degeneration. Spine J. 2005;5(6 Suppl):267S-279S.

57. Hunziker EB, Schenk RK, Cruz-Orive LM. Quantitation of chondrocyte performance in growth-plate cartilage during longitudinal bone growth. J Bone Joint Surg Am. 1987;69:162-73.

58. Bylski-Austrow DI, Wall EJ, Ballard ET, Kolata RJ, Glos DL, Sheyn D, Crawford AH. Spinal hemiepiphysiodesis induces physeal histomorphometric gradients. Trans Orthop Res Soc. 2005;30:1331.

59. Wilke HJ, Kettler A, Claes LE. Are sheep spines a valid biomechanical model for human spines? Spine. 1997;22:2365-74.

60. Bylski-Austrow DI, Glos DL, Sauser FE, Miller J, Jain V, Crawford A, Wall EJ. In vivo compressive stresses in the intervertebral disc vary in quadrupeds and are lower than human. Trans Orthop Res Soc. 2008;33:1329.

61. Glos DL, Sauser FE, Jain V, Crawford AH, Wall EJ, Bylski-Austrow DI. In vivo compressive stresses in the intervertebral disc vary in quadruped. Trans Orthop Res Soc. 2007;32:1057.

62. Charles YP, Daures JP, de Rosa V, Diméglio A. Progression risk of idiopathic juvenile scoliosis during pubertal growth. Spine. 2006;31:1933-42.

63. Diméglio A. Growth in pediatric orthopaedics. In: Morrissy RT, Weinstein SL, editors. Lovell and Winter's pediatric orthopaedics. 5th ed. Philadelphia: Lippincott Williams and Wilkins; 2001. p 33-62.

64. Stokes IA, Windisch L. Vertebral height growth predominates over intervertebral disc height growth in adolescents with scoliosis. Spine. 2006;31:1600-4.

65. Stokes IA, Spence H, Aronsson DD, Kilmer N. Mechanical modulation of vertebral body growth. Implications for scoliosis progression. Spine. 1996;21:1162-7.

66. Stokes IA, Burwell RG, Dangerfield PH; IBSE. Biomechanical spinal growth modulation and progressive adolescent scoliosis—a test of the 'vicious cycle' pathogenetic hypothesis: summary of an electronic focus group debate of the IBSE. Scoliosis. 2006;1:16.